Production, purification and characterization of an elastin-like polypeptide containing the Ile-Lys-Val-Ala-Val (IKVAV) peptide for tissue engineering applications

Bruno Paiva dos Santos, Bertrand Garbay, Mattia Pasqua, Elsa Chevron, Zoeisha Chinoy, Christophe Cullin, Katell Bathany, Sébastien Lecommandoux, Joelle Amedee, Hugo Oliveira, et al.

HAL Id: hal-02100654
https://hal.archives-ouvertes.fr/hal-02100654

Submitted on 16 Apr 2019

Production, purification and characterization of an elastin-like polypeptide containing the Ile-Lys-Val-Ala-Val (IKVAV) peptide for tissue engineering applications

Bruno Paiva dos Santos[1], Bertrand Garbay[2*], Mattia Pasqua[1], Elsa Chevron[1], Zoeisha S. Chinoy[2], Christophe Cullin[3], Katell Bathany[3], Sébastien Lecommandoux[2], Joëlle Amédée[1], Hugo Oliveira[1] and Elisabeth Garanger[2]

[1]Université de Bordeaux, 146 rue Léo Saignat, Bordeaux 33076, France, and INSERM, Bioingénierie Tissulaire (U1026, BioTis), Bordeaux, France

[2]Université de Bordeaux/Bordeaux INP, ENSCBP, 16 avenue Pey-Berland, Pessac 33607, France, and CNRS, Laboratoire de Chimie des Polymères Organiques (UMR5629, LCPO), Pessac, France

[3]Université de Bordeaux/Bordeaux INP, allée Geoffroy Saint Hilaire, Pessac 33600, France, and CNRS, Chimie et Biologie des Membranes et des Nano-objets (UMR5248, CBMN), Pessac, France

[*]Corresponding author. Tel: +33 540 006 693; Fax: +33 540 008 487

Corresponding author at: LCPO, UMR5629, ENSCBP, 16 avenue Pey-Berland, Pessac 33607, France

E-mail address: bertrand.garbay@bordeaux-inp.fr

Running title: IKVAV-ELP for neurotization
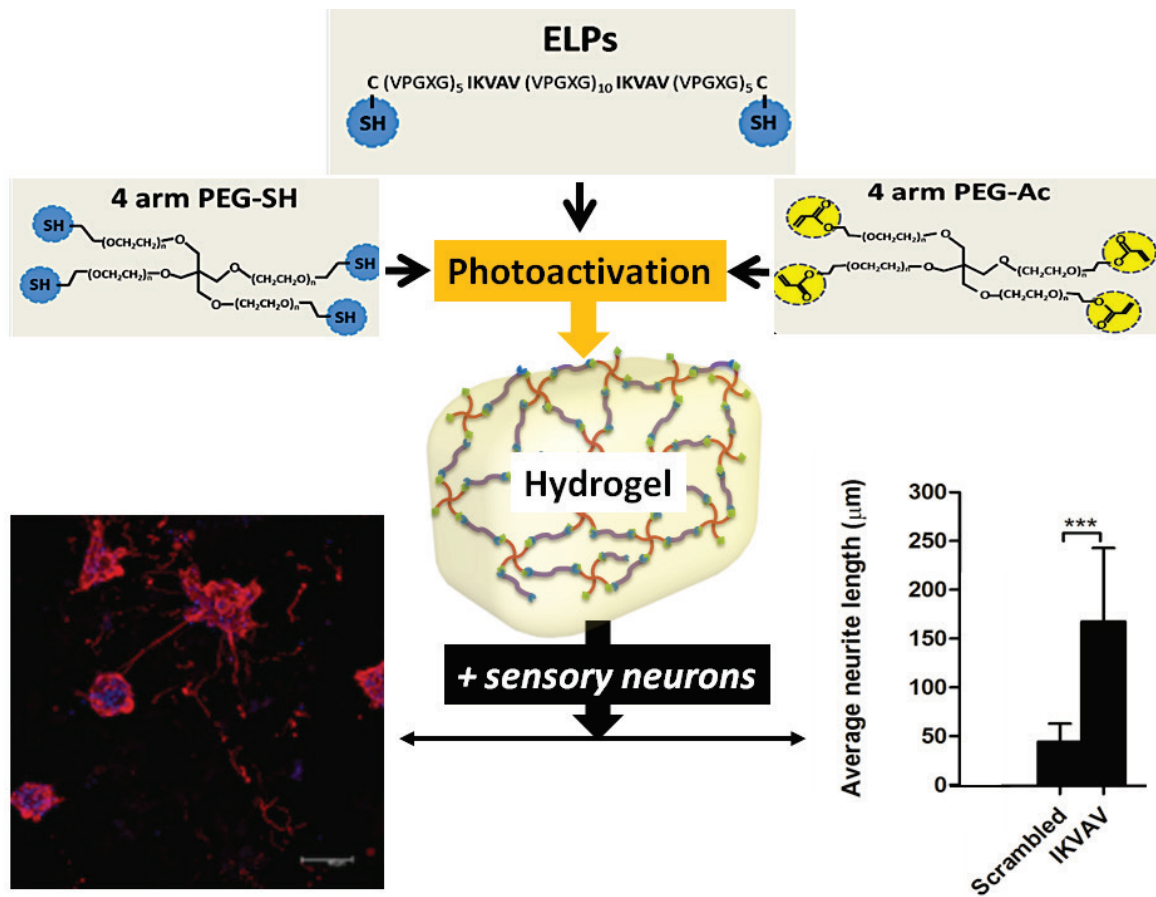
Abstract

Elastin-like polypeptides (ELPs) are biocompatible-engineered polypeptides, with promising interest in tissue engineering due to their intrinsic biological and physical properties, and their ease of production. The IKVAV (Ile-Lys-Val-Ala-Val) laminin-1 sequence has been shown to sustain neuron attachment and growth. In this study, the IKVAV adhesion sequence, or a scrambled VKAIV sequence, were incorporated by genetic engineering in the structure of an ELP, expressed in *Escherichia coli* and purified. The transition temperatures of the ELP-IKVAV and ELP-VKAIV were determined to be 23 °C. Although the phase transition was fully reversible for ELP-VKAIV, we observed an irreversible aggregation for ELP-IKVAV. The corresponding aggregates shared some characteristics with amyloid-like polypeptides. The two ELPs were then reacted with functionalized polyethylene glycol (PEG) to form hydrogels. These hydrogels were characterized for rheological properties, tested with cultures of rat primary sensory neurons, and implanted subcutaneously in mice for 4 weeks. Sensory neurons cultured on high IKVAV concentration hydrogels (20%) formed longer neurite than those of neurons grown on hydrogels containing the scrambled IKVAV sequence. Finally, *in vivo* evaluation showed the absence of detectable inflammation. In conclusion, this functionalized ELP-IKVAV biomaterial shows interesting properties for tissue engineering requiring neurotization.

Keywords

Abbreviations

1. Introduction

In any tissue-engineering application, the interaction of cells with the extracellular matrix is of major importance, as it supports the processes of cell adhesion, proliferation, migration and differentiation. In this sense, the development of biomaterials bearing guidance cues that can support these processes is fundamental in the establishment of novel, and more efficacious, tissue engineering applications. When considering for example bone tissue-engineering applications, where the effective reconstruction of large bone segments remains a major unsolved problem, two major processes have shown to be critical: angiogenesis and neurogenesis (Fukuda et al., 2013; Grellier, Bordenave, & Amédée, 2009; Guerrero et al., 2013; Jones, Mollano, Morcuende, Cooper, & Saltzman, 2004; Lee et al., 2012; Silva, Santos, Leng, Oliveira, & Amédée, 2017). As such, biomaterials development should consider the support of these processes. Additionally, when considering a clinical application, off the shelf, up-scalable and simpler biomaterial approaches may reduce regulatory, production and cost issues. Such an example relies on the use of elastin like polypeptides (ELPs). ELPs are recombinant peptide polymers, derived from the hydrophobic region of tropoelastin (Urry, Trapane, & Prasad, 1985), that consist of multiple repeats of Val-Pro-Gly-*Xaa*-Gly pentapeptides, where the guest residue (*Xaa*) can be any amino acid except proline. ELPs are characterized by an inverse transition temperature (Tt) (Li, Alonso, & Daggett, 2001; Urry, 1992). Below the Tt, the free polymer chains of ELPs remain disordered, fully hydrated and thus soluble in aqueous solution. Above the Tt, the ELP chains fold hydrophobically to form insoluble aggregates. This phenomenon is fully reversible, influenced by the nature of the guest residue *Xaa* (*e.g.* polar, charged, hydrophobic) and by the ELP chain length (Meyer & Chilkoti, 2004). It also depends on the polypeptide concentration, as well as on the nature and concentration of co-solutes. Recombinant ELPs are especially attractive for tissue

engineering as they can include cell specific sequences, they can be engineered to approach the viscoelastic properties of native elastin upon cross-linking, and they can be produced in large scale. In addition, they are biocompatible, biodegradable and can be purified using their inherent transition temperature without the need for complex and expensive chromatographic approaches (Changi et al., 2018; Nettles et al., 2010; Nicol et al., 1992; Prieto et al., 2011).

Several synthetic biomaterials were designed to incorporate signaling epitopes for cell-cell and cell-tissue interactions. A well-studied epitope is the short bioactive pentapeptide Ile-Lys-Val-Ala-Val (IKVAV), a motif derived from laminin, which has shown to promote neuron cell attachment, migration and neurite outgrowth (Nomizu et al., 1995; Silva et al., 2004). This pentapeptide can also increase endothelial cell mobilization, capillary branching and revascularization (Grant et al., 1992; Nakamura et al., 2008). This peptide was grafted to a number of different scaffolds such as aminated polymer surface (Santiago, Nowak, Rubin, & Marra, 2006), methacrylamide chitosan (Yu et al., 2007), collagen (Hosseinkhani et al., 2013; Li et al., 2014), or to a small dipeptide such as PA (Niece et al., 2008; Silva et al., 2004). It has been widely used in tissue engineering by immobilizing it onto hydrogel scaffolds (Drury and Mooney, 2003; Shekaran and Garcia, 2011; Zhu, 2010).

Here, we have used the inherent capabilities of ELPs for purification and for the inclusion of cell-specific sequences to produce recombinant peptide polymers, containing the IKVAV to form a hydrogel capable of supporting neurotization. We describe the (i) production, purification, and characterization of IKVAV-containing ELPs, (ii) the use of this engineered polypeptide as a functional component for hydrogel production, and (iii) the application of this new synthetic extracellular matrix in tissue engineering.

2. MATERIALS AND METHODS

2.1 Materials.

Enzymes required for recombinant DNA, including restriction endonucleases, OneTaq® hot start DNA polymerase, Antarctic phosphatase and Quick ligation™ kit (T4 DNA ligase) were obtained from New England Biolabs (NEB, Ipswich, MA, USA). The pET-44a(+) plasmid and the *E. coli* strain BLR(DE3) were obtained from Novagen Inc (Madison, WI, USA). Synthesis of the ELP-IKVAV and ELP-VKAIV genes were achieved by Eurofin MWG Operon (Ebersberg, Germany). All custom oligonucleotides were synthesized by Eurogentec (Seraing, Belgium). Sequencing of the different constructs was performed by GATC biotech (Cologne, Germany). All chemicals were from Sigma-Aldrich (Saint-Louis, MO, USA).

2.2 Construction of expression vector for ELP genes.

Synthetic genes corresponding to the ELP-IKVAV and ELP-VKAIV sequences (Figure 1) provided in pUC19 plasmid, were extracted from the said plasmid by a double digestion with *Nde*I and *Bam*HI, and the corresponding fragments were purified after agarose gel electrophoresis with the PCR clean-up, gel extraction kit (Macherey-Nagel GBMH, Düren, Germany). Purified fragments were ligated with the Quick ligation™ kit into similarly digested and dephosphorylated pET-44a(+). After transformation into *E. coli* BLR(DE3), transformants were selected by colony PCR with OneTaq® hot start DNA polymerase, and the primers pET-F (5'-TAATACGACTCACTATAGGG-3') and pET-R (5'-GTTATGCTAGTTATTGCTCAGCGG-3'). Plasmids from the positive clones were purified with the Plasmid DNA Purification kit (Macherey-Nagel, Düren, Germany) according to manufacturer's instructions, and verified by DNA sequencing.

2.3 Bioproduction of recombinant ELPs.

A single bacterial colony was selected and cultured overnight at 37°C in a rotary shaker at 200 rpm in 50 mL of rich LB medium (1% bacto tryptone, 0.5% NaCl, 1% yeast extract) containing 100 µg/mL ampicillin. Thereafter, this seed culture was inoculated into 150 mL of

LB-rich medium containing 100 µg/mL ampicillin. Cells were cultivated at 37 °C in a 500 mL baffled shake flask in a rotary shaker at 150 rpm. When the optical density at 600 nm (OD_{600nm}) reached a value close to 1.4, isopropyl β-D-thiogalactopyranoside (IPTG) was added to a final concentration of 0.3 mM, and the cultivation temperature was decreased to 25 °C.

2.4 Purification of recombinant ELPs.

After 21 h of IPTG induction, the OD_{600nm} of the cultures reached a value close to 4. Cells were harvested by centrifugation at 3,000 g and 4 °C for 15 min, and the cell pellet was resuspended with 10 mL/g wet weight in PBS buffer (NaCl 137 mM, KCl 2.7 mM, Na_2HPO_4 8 mM, KH_2PO_4 2 mM, pH 7.4) supplemented with one tablet/10 mL of Complete Mini EDTA-free protease inhibitors (Roche, Basel, Switzerland). Thereafter, samples were incubated for 4 h at -80 °C, and thawed by incubation at 10 °C. Total cell lysis was performed by sonication for 10 min at 12 °C with several 4-second pulses at 125 W, 8 seconds apart. Then, the homogenates were centrifuged at 3,000 g and 4 °C for 15 min. For ELP-VKAIV, the supernatant was directly used for the polypeptide purification by four successive rounds of inverse transition cycling (ITC) (Meyer & Chilkoti, 1999). Briefly, the ELP was precipitated at 37 °C in the presence of 1 M NaCl, and pelleted by centrifugation at 10,000 g and 25 °C for 10 min ("Hot Spin"). After elimination of the supernatant containing soluble proteins and re-suspension of the pellet in cold PBS buffer, the ELP was re-dissolved whereas insoluble proteins from *E. coli* were eliminated by centrifugation for 10 min at 10,000 g and 4 °C ("Cold Spin"). The supernatant containing the ELP was then processed through successive ITC cycles. NaCl was not added to the sample after the first round of ITC.

In the case of ELP-IKVAV, the 3,000 g pellet was re-suspended in 20 mL cold-PBS supplemented with β-mercaptoethanol at a final concentration of 0.68 M. After an overnight

incubation at 4 °C on a rotary agitator, the homogenate was centrifuged at 3,000 g and 4 °C

for 15 min, and the supernatant was subjected to three successive rounds of ITC purification

as described above. Finally, the purified ELPs were dialyzed against ultrapure water at 4 °C

in dialysis membranes with a 3.5-kDa cutoff (Slide-A-Lyer®Mini Dialysis Devices, Thermo

Scientific, Rockford, IL, USA) for five hours. After a final overnight dialysis, samples were

stored at -20°C. Protein content of the purified fraction was determined by spectrophotometry

at 280 nm with a Nanodrop (NanoDrop-ND 1000). Due to their low Tt, the samples

aggregated rapidly at room temperature. Therefore, they should first be diluted with ethanol

(70% final concentration) and kept on ice until the measurement. Parameters for the

Nanodrop were set at 5,500 for the extinction molar coefficient, and at 10,180 Da for the

molecular mass.

2.5 Chemical and physico-chemical characterization of ELPs.

The molecular mass of each purified ELP was determined by matrix-assisted laser

desorption/ionization mass spectrometry (MALDI-MS). Analyses were performed on a

MALDI-ToF-ToF (Ultraflex III, Bruker Daltonics, Bremen, Germany) equipped with a

SmartBeam laser (Nd:YAG, 355nm). Samples at a final concentration of 0.5 mg/mL were

mixed with the matrix sinapinic acid (Sigma Aldrich) at 10 mg/mL in acetonitrile/0.1%

aqueous TFA (1/1, v/v). All MALDI-MS measurements were acquired in the linear positive

mode and a mixture of standard proteins (Sigma-Aldrich, Saint-Louis, MO, USA) was used

for external calibration covering the mass range from 8,500 Da to 17,000 Da.

The transition temperatures of ELPs at two different concentrations in PBS solution were

determined by measuring the turbidity at 350 nm between 10 and 40 or 50 °C, at 1 °C min^{-1}

scan rate. Data were collected on a Cary 100 Bio UV−visible spectrophotometer equipped

with a multi-cell thermoelectric temperature controller from Varian (Palo Alto, CA). The Tt

was defined as the temperature corresponding to the maximum of the first derivative of the turbidity versus temperature curve (Christensen et al., 2013).

2.6 Analysis of ELP-IKVAV aggregates

Amyloid-like fibril formation was monitored by thioflavin T (ThT) binding. Fluorescence emission of 20 µM ThT was measured in the presence of 150 µM ELP in PBS with a POLAR star Omega microplate reader (BMG Labtech, Champigny-sur-Marne, France). Excitation at 440-448 nm, and emission spectrum was recorded between 460 and 550 nm. Samples were preincubated at 4°C prior to the analysis to prevent gel formation in the wells.

2.7 Hydrogel production and rheology

PEG gels were composed of 4 arm thiol-ended PEG (SH-PEG, 20 kDa) (JenKem, USA), 4 arm acrylate PEG (Ac-PEG), at thiol to acrylate equimolar ratios. Photopolymerization was achieved using the photoinitiator Irgacure® 2959 (0.5% w/v) exposure to UV light (λ=305 nm) following a thiol-ene click Michael addition. Different mass ratios of ELPs and PEG were explored to attain optimal rigidity and appropriate sensory neuron attachment and neurite outgrowth. Briefly SH-PEG was substituted by ELPs at different mass rations. Namely: (i) 50% (w/w) of Ac-PEG + 45% (w/w) of SH-PEG + 5 (w/w) of ELP, (ii) 50% (w/w) of Ac-PEG + 40% (w/w) of SH-PEG + 10% (w/w) of ELP and (iii) 50% (w/w) of Ac-PEG + 30% (w/w) of SH-PEG + 20% (w/w) of ELP.

The rheological properties of the hydrogels were evaluated upon 24 h of soaking in PBS by determining the frequency dependence of the storage (G') and loss moduli (G"). Frequency sweeps were performed at a constant strain (0.1) in the angular frequency range 0.1–100 rad s^{-1}. This characterization was performed for the composite hydrogels (containing ELPs) at a

final concentration of 15% (w/v) while varying the ELP concentration in the final hydrogel mass (*i.e.* 5%, 10% and 20% (w/w)). Measures were performed at 4 and 37 °C.

2.8 Cell isolation, culture, and characterization

Primary sensory neurons were obtained from dorsal root ganglion from healthy 6-10 week-old Wistar rats as described elsewhere (Malin et al., 2007). Briefly, spinal columns was removed and opened from the caudal to the rostral in order to expose the dorsal root ganglions. They were individually harvested and digested with 1 mg/mL Collagenase Type IV (Gibco®) for 2 h at 37 °C. Subsequently, the digestion product was washed twice with culture medium supplemented with 2% (v/v) B-27 Serum-Free Supplement® (B-27, Gibco®), and 1% (v/v) Penicilin-Streptomycin, and mechanically dissociated using fire polished glass Pasteur pipettes (full diameter and ½ diameter). The cell suspension was finally washed three times with medium and resuspended in culture medium. The culture medium was supplemented with 1 µM cytarabine, to avoid the proliferation of the Schwann cells that were present in the primary culture.

Sensory neurons previously cultured on 100 µg/mL poly-D-lysine- and 10 µg/mL laminin-coated coverslips for 7 days, were fixed in 1% (w/v) paraformaldehyde (PFA, Merck Millipore, Darmstadt, Germany) for 10 min at room temperature, washed once with PBS 0.1 M and permeabilized for 5 min with 0.1% (v/v) Triton® X-100 (EDM Millipore, Bilerica, MA, USA). A 1% (w/v) bovine serum albumin (BSA) solution was used for antigen blocking for 30 min at room temperature to minimize the non-specific binding. Goat anti- rat calcitonin gene-related peptide antibody (CGRP, 1:50; Abcam, Cambridge, UK) was used as primary antibody overnight at 4 °C and Alexa Fluor® 488-conjugated chicken anti-goat secondary antibody (1:250; Molecular Probes®, Life Technologies) was used as secondary

antibody for 1 h at room temperature. Photomicrographies were taken using laser-scanning microscope (SPE, Leica Microsystems).

2.9 Neurite length evaluation

Sensory neurons were seeded on hydrogels at 20,000 cells per square cm and cultivated for 7 days. Subsequently, cells were fixed with 4% (w/v) paraformaldehyde at 4 °C for 30 min, permeabilized with Triton X-100 at 0.1% (v/v) for 30 min at 4 °C and blocked with BSA 1% (w/v) for 1 h. Primary antibody rabbit anti-rat beta III Tubulin (Abcam) was used at a dilution 1:500 overnight at 4 °C and second antibody goat anti-rabbit IgG conjugated with Alexa Fluor 568 (Molecular probes) at 1:200 dilution for 2 h at room temperature. Nuclei were labeled with DAPI (4', 6'-diamidino-2-phenylindole, FluoProbes) at 1 µg/mL for 30 min at room temperature. Sensory neurons morphology was visualized using a confocal laser-scanning microscope (SPE, Leica Microsystems). The quantification of the neurite length was performed using Image J, using "Simple Neurite Tracer" tool. Neurites were measured tracing a path from the soma to the visible end and the length was converted in µm (n>4).

2.10 Subcutaneous hydrogel implantation

Balb/c mice (n=4 for each group) housed in the animal care facility of the 4A building of the University of Bordeaux (Bordeaux, France) were used for the in vivo evaluations. They were under conditions of circadian day-night rhythm, and they were fed ad libitum. Animal experimentation protocol was approved by the local Ethic Committee (protocol n° APAFIS #4375-2016030408537165 v4).

15% (w/v) hydrogels containing IKVAV, or the scrambled adhesion sequence, were produced in 96 wells in a volume of 50 µL and were implanted subcutaneously at the medio-dorsal position in sterile conditions. After 28 days of implantation, mice were euthanized in a

CO_2 chamber and samples with the surrounding tissue were collected and extensively rinsed with PBS 0.1 M (pH 7.4) and then fixed with 4% (w/v) PFA for 30 min at 4 °C. Sections of 10 μm thickness were obtained using a cryostat (Leica CM 1850 UV). Haematoxylin and eosin staining was performed under standard conditions, slides were then mounted using Clearmount medium (Invitrogen, USA).

2.11 Statistical analysis

Using the Graphpad Prism 5.0 Software, a D'Agostino and Pearson normality test was used in order to test if values obeyed to a Gaussian distribution. Statistically significant differences between several groups were analyzed by the non-parametric Kruskal-Wallis test, followed by a Dunns post-test. A p-value lower than 0.05 was considered to be statistically significant.

3. Results and discussion

3.1 Design of the ELPs

We have designed an ELP-based recombinant polymer with interspersed sequences of VPGVG (n = 8), VPGIG (n = 8) and VPGMG (n = 4). The gene sequence was selected according to *E. coli* codon usage while minimizing sequence repetition (Figure 1). We incorporated two sequences of the pentapeptide epitope IKVAV (or its scrambled version VKAIV) in the ELP backbone. Thus, ELP-IKVAV and ELP-VKAIV have identical MW (10,189 Da), theoretical pI (8.89), and grand average of hydropathicity (GRAVY, 1.236). Tryptophan was included to monitor ELP during the final step of the purification process thanks to its UV absorption. Two cysteine residues were added close to the *N*-terminus and *C*-terminus of the ELP for subsequent cross-linking purposes and post-polymerization modifications (Xu et al., 2012; Zhang et al., 2015). Other post-production modifications

could be performed at the methionine residues, as recently demonstrated (Kramer et al., 2015). The GenBank accession numbers are **KU743475** and **KU743476**, for ELP-IKVAV and ELP-VKAIV, respectively.

3.2 Production and purification of ELPs

In typical experiments, bacteria were cultivated at 37 °C in LB medium until OD_{600nm} reached a value around 1.4. IPTG was then added to a final concentration of 0.3 mM, and the cultivation temperature was decreased to 25 °C. In a first series of experiments, the time-course accumulation of the two ELPs was monitored by SDS-PAGE. A band corresponding to the expected ELPs was detected 2 h after IPTG addition, and its amount increased up to 21 h of culture (data not shown). This duration of culture post-induction was thus selected for all the following experiments. After cell lysis, the homogenate was centrifuged at 3,000 g, and proteins from the corresponding pellet and supernatant were analyzed by gel electrophoresis. The result from a typical experiment is shown in Figure 2. For the two ELPs, a band migrating slightly lower than the 10 kDa protein marker was detected in the induced culture when compared to the non-induced one. This apparent MW is compatible with the one expected for the two ELPs, namely ELP-IKVAV and ELP-VKAIV. However, these two polypeptides behaved differently during the purification process. The ELP-IKVAV was predominantly retrieved in the 3,000 g pellets, suggesting that it mainly accumulated in the form of insoluble aggregates. To check that no substantial amount of ELP-IKVAV was present in the supernatant, we performed one round of ITC purification with this soluble fraction, and no significant amount of ELP-IKVAV was recovered in the final "cold spin" supernatant (Figure S1). On the contrary, substantial amounts of ELP-VKAIV were present in the 3,000 g supernatant, although some was present in the pellet. Indeed, densitometry analysis of this gel showed that 69% of ELP-VKAIV was in the soluble fraction. The fact that ELP-IKVAV and ELP-VKAIV exhibited different solubility was quite unexpected

because they possess identical physico-chemical characteristics (MW, pI, GRAVY index, cysteine content).

We then sought after a solubilization method for the ELP-IKVAV protein product. Several strategies were described to prevent the formation of insoluble aggregates during recombinant expression in *E. coli*. Their goal is usually to diminish the synthesis rate of the recombinant protein. Indeed, we did several experiments where the final concentration of IPTG was decreased from 0.5 mM to 0.3 mM, and then 0.1 mM, but this did not result in an increase in the ELP-IKVAV solubility. We also decreased the temperature of the culture after the induction by IPTG from 37°C to 30°C, 25°C or 20°C with no more success. We therefore sought for a solution to solubilize the polypeptide from the 3,000 g pellet obtained after cell lysis. Multiple buffers can be used to enhance protein solubility (Bondos and Bicknell, 2003). We chose to test the chaotrope urea (8 M final concentration), the detergent *N*-Lauroylsarcosine (14.6 mM final concentration) and the reducing agent β-mercaptoethanol (0.68 M final concentration). The latter was evaluated because both ELPs contained two cysteine residues that may trigger aggregation throughout the formation of intra- or inter-molecular disulfide bridges. In all cases, fractions of the pellet 3,000 g were incubated overnight at 4 °C, centrifuged at 3,000 g, and the efficiency of solubilization was assessed by SDS-PAGE analysis of the supernatant and pellet fractions (Figure S2). This experiment showed that *N*-Lauroylsarcosine was inefficient at solubilizing ELP-IKVAV from the 3,000 g pellet. On the contrary, 90% of this polypeptide was recovered in the 3,000 g supernatant after treatment by 8 M urea. However, when ITC purification was performed with the corresponding soluble fraction, the majority of ELP-IKVAV did not precipitate during the hot spin step and was therefore lost in the supernatant. For some reason, urea somewhat prevented the coacervation that should occur when the ELP is placed at a temperature above its *T*t. After one ITC round of purification, only trace amounts of the polypeptide could be

recovered (Lane SCS, Figure S2). The profound effect of urea on the coacervation temperature of ELP has already been reported (Miao et al., 2005). Finally, the best results were obtained with β-mercaptoethanol. After an overnight incubation with this reducing agent, 58% of the ELP-IKVAV was solubilized from the initial 3,000 g pellet. More importantly, only trace amounts were lost in the hot spin supernatant or in the cold spin pellet during the ITC cycle (Figure S2). We thus decided to use β-mercaptoethanol to purify ELP-IKVAV in the following experiments. Indeed, starting with the supernatant post-β-mercaptoethanol treatment (lane 3, Figure 3), we were able to purify to homogeneity the ELP-IKVAV by three successive rounds of ITC (Figure 3). To achieve good purity, four rounds of ITC were necessary for ELP-VKAIV because more proteins were present in the initial fraction (supernatant 3,000 g post-lysis, see lane 5, Figure 3). It should be noted that an additional band around 20 kDa MW was present in the two purified samples. This band corresponds in size to ELP dimers, which were quite resistant to the β-mercaptoethanol present in the sample loading buffer. Interestingly, SDS-PAGE performed in non-reducing conditions showed that numerous multimers (ranging from dimer to heptamer) were present in the two ELP purified fractions (Figure S3). The presence of multimers in the purified ELP-IKVAV sample was rather unexpected because this polypeptide was extracted from the 3,000 g insoluble pellet by using 0.68 M β-mercaptoethanol. This suggests that the formation of the intermolecular disulfide bridges occurred during the ITC cycles and/or during the dialysis step. For the two ELPs, the yield of the purified protein was 95 ± 25 mg/L (n=6). This yield was significantly higher than those previously obtained in our laboratory for hydrophobic ELPs (Bataille et al., 2016, 2015).

3.3 Physico-chemical characterization of ELPs

The molecular mass of each purified ELP was determined by matrix-assisted laser desorption/ionization mass spectrometry (Figure S4). The average masses measured by

MALDI-MS were 10,055.2 Da and 10,054.6 Da for ELP-IKVAV and ELP-VKAIV, respectively. With the theoretical molecular weight being 10,189.4 Da, the likely hypothesis to explain the mass difference between the experimental and theoretical values (~134 Da) is that the *N*-terminal Met (131.2 Da) was excised from the polypeptides by methionine amino peptidase during the production in *E. coli* (Ben-Bassat et al., 1987). Indeed, the *N*-terminal methionine is often cleaved off when the second residue in the primary sequence is small and uncharged (Hirel et al., 1989), which is the case for our ELPs with a cysteine residue following the initial methionine.

The thermal behavior of the two ELPs was studied by turbidimetry. A first series of experiments showed that the amount of multimers in the sample, which results from the formation of intermolecular disulfide bridges, dramatically affected the phase transition of the ELP. Indeed, *T*ts were measured for the same ELP-VKAIV sample which was either untreated, heated for 10 min at 95°C to increase aggregation (Kaneko and Kitabatake, 1999), or treated with β-mercaptoethanol (Figure 4). For the three samples, we observed a sharp single transition as expected for ELP monoblocks. The relative amounts of the multimeric species present in each sample was evaluated by SDS-PAGE analysis (insert of Figure 4). The *T*t measured, respectively at 18°C (untreated), 14°C (pre-heated) and 23°C (reduced), were inversely correlated to the proportion of multimers, the *T*t decreasing when the amount of multimers increased. This result was expected because it has been previously demonstrated that the *T*t of a given ELP is inversely related to its molecular mass (Meyer & Chilkoti, 2004). A similar conclusion could be drawn for ELP-IKVAV (Figure S5).

Taking into account the formation of intermolecular disulfide bridges, we chose to measure the *T*ts in the presence of 0.68 M β-mercaptoethanol to favor the presence of monomers because it was not possible to precisely control the state of multimerization between different samples.

One of the hallmarks of the ELP is that the transition from the soluble form to the insoluble and aggregate state is reversible (Urry et al., 1985). We therefore investigated the reversibility of the ELP-IKVAV and ELP-VKAIV solutions. To achieve this goal, the same solution of ELP was submitted to two consecutive runs of thermal denaturation (Figure 5). This experiment showed that the ELP-VKAIV behaved like a typical ELP, with a transition around 23 °C that was measured during the two successive experiments. On the contrary, the ELP-IKVAV showed a classical turbidity profile during the first run, but the aggregates that were formed above the Tt did not disintegrate when the temperature was lowered below 15 °C, and therefore the turbidity remained constant during the second experiment. This unexpected phenomenon did not result from the presence of intermolecular disulfide bridges because the experiment was performed in the presence of the reducing agent β-mercaptoethanol. In addition, such irreversibility was not seen for the ELP-VKAIV, which contains also two cysteine residues, and therefore the same capacity for multimerization. The irreversibility of the transition was thus attributed to the presence of the IKVAV motifs in the ELP sequence. It should be noted that prolonged incubation of the solution of aggregated ELP-IKVAV at 4° C did not allow solubilization of the said ELP.

3.4 Insights into the insolubility of ELP-IKVAV

The difference in solubility between the two ELPs was difficult to understand. As previously stated, they have an identical amino acid composition and MW. Both contain two cysteine residues. The fact that β-mercaptoethanol enhanced the solubility of ELP-IKVAV during the purification process, suggests that the formation of intra- or inter-molecular disulfide bridges plays a role in the aggregation of the said polypeptide, but an additional mechanism is very likely to take place. Indeed, the same intra- or intermolecular disulfide bridges may be formed during the production of the ELP-VKAIV, but this ELP was mainly soluble (see Figure 2). In addition, turbidity measurements clearly showed that the aggregation of ELP-

IKVAV was irreversible, whereas the transition of ELP-VKAIV was fully reversible. In fact, it has already been reported that a 12-mer peptide containing the IKVAV motif (called LAM-L) formed amyloid-like fibrils, whereas peptides containing a scrambled IKVAV motif did not (Yamada et al., 2002). To test this hypothesis, samples of the two ELPs, each at a concentration of 150 μM, were incubated at 25 °C in the absence of β-mercaptoethanol. As expected, a gel rapidly formed in the two tubes as the temperature was above the Tt of the ELPs. However, after overnight incubation at 37 °C, a coacervate was still visible in the ELP-VKAIV tube whereas a precipitate accumulated at the bottom of the ELP-IKVAV tube. In this case, the gel structure collapsed and the ELP sedimented under the form of macroscopic aggregates (Figure S6). A similar phenomenon occurred when a similar sample was incubated for three days at 4°C.

To investigate if these aggregates contain amyloid-like structures, we used a specific test based on the binding of thioflavin T (ThT) (Biancalana and Koide, 2010; Khurana et al., 2005). We analyzed samples from ELP-IKVAV stored at -20 °C, or those stored at 4 °C for three days. A sample from ELP-VKAIV stored at 4 °C for three days was used as a control (Figure 6). A strong characteristic fluorescence signal at 482 nm was observed for the ELP-IKVAV sample, upon storage for three days at 4 °C. The signal was significantly lower for an ELP-VKAIV sample stored under the same conditions, or for an ELP-IKVAV sample stored at -20 °C and carefully defrost on ice just before the measurement. Using this test, we can conclude that the aggregates obtained after incubation of ELP-IKVAV at 4 °C possessed some characteristics of amyloid-like fibrils (*i.e.* rich in ß-strand secondary structures), and that these entities were not present in significant quantities when the same sample was stored at -20 °C or in the ELP-VKAIV sample.

3.5 Hydrogel production

Since we aimed to produce hydrogels to contemplate neurotization and vascularization, we targeted a hydrogel with storage modulus (G') between 1 kPa and 1.5 kPa. Indeed, this range of substrate stiffness has shown to be optimal for dorsal root ganglia (DRG) neurons outgrowth (Koch et al., 2012). Preliminary experiments showed that hydrogels obtained by crosslinking pure monomers of ELP-IKVAV or ELP-VKAIV do not meet this criterion. Therefore, we chose to use poly(ethylene glycol) (PEG) as a crosslinking agent to enhance the rheological properties. PEG is currently FDA-approved for several medical applications and presents several characteristics that favor its use in biomedical applications, such as low toxicity, low protein adsorption, and low immunogenicity. Albeit PEG is slowly biodegradable, it has been shown that PEGs with a molar mass below 20 kDa are easily excreted in urine (Pasut and Veronese, 2007). Moreover, it has already been shown that the ELP-PEG hydrogels have substantially improved optical transparency compared with pure ELP hydrogels, which facilitate *in vitro* analyses (Wang et al., 2014).

As means to achieve the production of PEG-ELP hydrogels, we used equimolar ratios of thiol to acrylate groups at different final polymer concentrations. Rheological analyses were performed to assess the storage (G') and loss (G'') moduli. Preliminary experiments showed that PEG gels made of 15% polymer with equimolar ratios of thiol to acrylate groups had a (G') value of 1.4 kPa. Then, further analyses were conducted using the 15% (w/v) final concentration hydrogel composition where we substituted the thiol PEG by different mass percentages of ELP-IKVAV, namely 5%, 10% and 20% (w/w). Composite hydrogels showed distinct behavior depending on the measurement temperature and on the percentage of ELP composition (Figure 7). At 4 °C, below the ELPs transition temperature, the composite gels showed a reduction of the elastic modulus (G'), more relevant for the higher ELP compositions. Conversely, the transition from 4 to 37 °C, resulted in an increase of the storage modulus of + 8%, + 67% and +78 %, for the 5, 10 and 20% (w/w) ELP hydrogels,

respectively. Similar results were obtained with the ELP-VKAIV hydrogel (Figure S7). This behavior can be explained by the inherent transition temperature of the polymers, ELP chains being soluble and fully extended below the Tt value. In response to strain, force is transmitted largely through these extended chains and chemical crosslinks. In addition, the polypeptide chains do not have much contact with each other (Trabbic-Carlson, Setton, & Chilkoti, 2003). At higher temperature, ELP chains are insoluble and contracted, decreasing water retention and increasing their intermolecular interactions, resulting in a tighter hydrogel network. As expected, these intermolecular interactions are proportional to the ELP concentration (Trabbic-carlson et al., 2003).

3.6 Evaluation of neurite growth on the hydrogels

Sensory neurons primary cultures were characterized by confocal microscopy through CGRP and β III tubulin immunostaining. Cells expressed CGRP in the cell body and neurite, and β III tubulin labelling was used to monitor neurite formation (Silva, Santos, Leng, Oliveira, & Amédée, 2017). In order to evaluate the capacity of the IKVAV-containing hydrogels to support neurite growth, we evaluated the behaviour of sensory neurons after 7 days of culture. As shown in Figure 8A, initial sensory neurons adhesion was observed for all the conditions studied. In scrambled peptide formulations, sensory neurons formed larger cellular aggregates with neurite wrapped around the cell bodies. Sensory neurons showed more dispersed cellular distribution and longer neurite when grown on IKVAV-containing hydrogels. Image analysis for average neurite length confirmed that hydrogels containing the highest IKVAV concentration (20% w/w) had longer neurite (168 ± 75 µm) relative to the same scrambled concentration (45 ± 19 µm, p < 0.001) (Figure 8B). The average neurite length for the 20% (w/w) IKVAV containing gels is similar to those previously published for adult rat sensory neurons grown for 7 days in the absence of nerve growth factor (NGF). Indeed, Kim and collaborators studied the effect of several growth factors on sensory neurons

isolated from adult rats, grown on collagen hydrogels for 7 days (Kim, Caspar, Shah, & Hsieh, 2015). They showed that the neurite length reached 229 ± 102 μm in the absence of NGF. In our study, we deliberately chose to evaluate the sensory neurons growth in the absence of supraphysiological concentrations of NGF, as means to analyze the particular impact of the hydrogel structure and to reflect the *in vivo* scenario, where adult cells from peripheral tissues can secrete neurotrophic factors that support neurotisation (Madduri and Gander, 2010; Wilkins et al., 2009).

3.7 *In vivo* evaluation of cytotoxicity

Based on the results obtained *in vitro*, 50 μL of hydrogels containing 20% (w/w) of ELP-IKVAV, or the scrambled sequence, were implanted subcutaneously in Balb/c mice (n=4 for each group). After 4 weeks, the samples were collected with the surrounding tissue and analyzed histologically (Figure 9). For both compositions, the implanted material was integrated in the surrounding tissue with a thin layer of fibrous tissue formed around the implanted material. These observations, coupled with the absence of any major inflammatory response, suggest a suitable biocompatibility for our material *in vivo*. This supports previous reports showing that ELP-based hydrogels do not trigger important cytotoxicity or inflammatory response after their *in vivo* implantation (Ibáñez-Fonseca et al., 2018; Nettles et al., 2008; Testera et al., 2015; Zhang et al., 2015).

4. Conclusion

We designed, produced, purified and characterized a recombinant ELP containing the IKVAV adhesion peptide, and formulated it with PEG to obtain biofunctional hydrogels. This approach allowed the modulation of both the mechanical properties and the density of the biologically relevant adhesion sequence, relevant for the optimal cell response. These hydrogels supported sensory neurons growth, triggered neurite lengthening, and showed good

biocompatibility after *in vivo* implantation. These features make the IKVAV-containing ELP hydrogels a promising engineered construct to be used as extracellular matrix in biomedical applications with a special need for neurotization.

Acknowledgements

References

Bataille, L., Dieryck, W., Hocquellet, A., Cabanne, C., Bathany, K., Lecommandoux, S., Garbay, B., Garanger, E., 2016. Recombinant production and purification of short hydrophobic Elastin-like polypeptides with low transition temperatures. Protein Expr. Purif. 121, 81–87. https://doi.org/10.1016/j.pep.2016.01.010

Bataille, L., Dieryck, W., Hocquellet, A., Cabanne, C., Bathany, K., Lecommandoux, S., Garbay, B., Garanger, E., 2015. Expression and purification of short hydrophobic elastin-like polypeptides with maltose-binding protein as a solubility tag. Protein Expr. Purif. 110, 165–171. https://doi.org/10.1016/j.pep.2015.03.013

Ben-Bassat, A., Bauer, K., Chang, S.Y., Myambo, K., Boosman, A., Chang, S., 1987. Processing of the initiation methionine from proteins: properties of the Escherichia coli methionine aminopeptidase and its gene structure. J. Bacteriol. 169, 751–7.

Biancalana, M., Koide, S., 2010. Molecular mechanism of Thioflavin-T binding to amyloid fibrils. Biochim. Biophys. Acta 1804, 1405–12. https://doi.org/10.1016/j.bbapap.2010.04.001

Bondos, S.E., Bicknell, A., 2003. Detection and prevention of protein aggregation before, during, and after purification. Anal. Biochem. 316, 223–231. https://doi.org/10.1016/S0003-2697(03)00059-9

Changi, K., Bosnjak, B., Gonzalez-Obeso, C., Kluger, R., Rodríguez-Cabello, J.C., Hoffmann, O., Epstein, M.M., 2018. Biocompatibility and immunogenicity of elastin-like recombinamer biomaterials in mouse models. J. Biomed. Mater. Res. Part A 106, 924–934. https://doi.org/10.1002/jbm.a.36290

Christensen, T., Hassouneh, W., Trabbic-Carlson, K., Chilkoti, A., 2013. Predicting transition temperatures of elastin-like polypeptide fusion proteins. Biomacromolecules 14, 1514–1519. https://doi.org/10.1021/bm400167h

Drury, J.L., Mooney, D.J., 2003. Hydrogels for tissue engineering: scaffold design variables and applications. Biomaterials 24, 4337–4351. https://doi.org/10.1016/S0142-9612(03)00340-5

Fukuda, T., Takeda, S., Xu, R., Ochi, H., Sunamura, S., Sato, T., Shibata, S., Yoshida, Y., Gu, Z., Kimura, A., Ma, C., Xu, C., Bando, W., Fujita, K., Shinomiya, K., Hirai, T., Asou, Y., Enomoto, M., Okano, H., Okawa, A., Itoh, H., 2013. Sema3A regulates bone-mass accrual through sensory innervations. Nature 497, 490–3. https://doi.org/10.1038/nature12115

Grant, D.S., Kinsella, J.L., Fridman, R., Auerbach, R., Piasecki, B.A., Yamada, Y., Zain, M., Kleinman, H.K., 1992. Interaction of Endothelial-Cells With a Laminin-a Chain Peptide (Sikvav) Invitro and Induction of Angiogenic Behavior Invivo. J. Cell. Physiol. 153, 614–625. https://doi.org/10.1002/jcp.1041530324

Grellier, M., Bordenave, L., Amédée, J., 2009. Cell-to-cell communication between

osteogenic and endothelial lineages: implications for tissue engineering. Trends Biotechnol. 27, 562–71. https://doi.org/10.1016/j.tibtech.2009.07.001

Guerrero, J., Catros, S., Derkaoui, S.-M., Lalande, C., Siadous, R., Bareille, R., Thébaud, N., Bordenave, L., Chassande, O., Le Visage, C., Letourneur, D., Amédée, J., 2013. Cell interactions between human progenitor-derived endothelial cells and human mesenchymal stem cells in a three-dimensional macroporous polysaccharide-based scaffold promote osteogenesis. Acta Biomater. 9, 8200–13. https://doi.org/10.1016/j.actbio.2013.05.025

Hirel, P.H., Schmitter, M.J., Dessen, P., Fayat, G., Blanquet, S., 1989. Extent of N-terminal methionine excision from Escherichia coli proteins is governed by the side-chain length of the penultimate amino acid. Proc. Natl. Acad. Sci. U. S. A. 86, 8247–51.

Hosseinkhani, H., Hiraoka, Y., Li, C.H., Chen, Y.R., Yu, D.S., Hong, P. Da, Ou, K.L., 2013. Engineering three-dimensional collagen-IKVAV matrix to mimic neural microenvironment. ACS Chem. Neurosci. 4, 1229–1235. https://doi.org/10.1021/cn400075h

Ibáñez-Fonseca, A., Ramos, T.L., González de Torre, I., Sánchez-Abarca, L.I., Muntión, S., Arias, F.J., del Cañizo, M.C., Alonso, M., Sánchez-Guijo, F., Rodríguez-Cabello, J.C., 2018. Biocompatibility of two model elastin-like recombinamer-based hydrogels formed through physical or chemical cross-linking for various applications in tissue engineering and regenerative medicine. J. Tissue Eng. Regen. Med. 12, e1450–e1460. https://doi.org/10.1002/term.2562

Jones, K.B., Mollano, A. V, Morcuende, J. a, Cooper, R.R., Saltzman, C.L., 2004. Bone and brain: a review of neural, hormonal, and musculoskeletal connections. Iowa Orthop. J.

24, 123–132.

Kaneko, R., Kitabatake, N., 1999. Heat-Induced Formation of Intermolecular Disulfide

Linkages between Thaumatin Molecules That Do Not Contain Cysteine Residues. J.

Agric. Food Chem. 47, 4950–4955. https://doi.org/10.1021/jf990267l

Khurana, R., Coleman, C., Ionescu-Zanetti, C., Carter, S.A., Krishna, V., Grover, R.K., Roy,

R., Singh, S., 2005. Mechanism of thioflavin T binding to amyloid fibrils. J. Struct. Biol.

151, 229–238. https://doi.org/10.1016/j.jsb.2005.06.006

Kim, H., W. Caspar, T., Shah, S.B., Hsieh, A.H., 2015. Effects of proinflammatory cytokines

on axonal outgrowth from adult rat lumbar dorsal root ganglia using a novel three-

dimensional culture system. Spine J. 15, 1823–1831.

https://doi.org/10.1016/J.SPINEE.2015.03.017

Kimberly Trabbic-Carlson, Lori A. Setton, and, Chilkoti*, A., 2003. Swelling and

Mechanical Behaviors of Chemically Cross-Linked Hydrogels of Elastin-like

Polypeptides. https://doi.org/10.1021/BM025671Z

Koch, D., Rosoff, W.J., Jiang, J., Geller, H.M., Urbach, J.S., 2012. Strength in the periphery:

growth cone biomechanics and substrate rigidity response in peripheral and central

nervous system neurons. Biophys. J. 102, 452–60.

https://doi.org/10.1016/j.bpj.2011.12.025

Kramer, J.R., Petitdemange, R., Bataille, L., Bathany, K., Wirotius, A.L., Garbay, B.,

Deming, T.J., Garanger, E., Lecommandoux, S., 2015. Quantitative Side-Chain

Modifications of Methionine-Containing Elastin-Like Polypeptides as a Versatile Tool

to Tune Their Properties. ACS Macro Lett. 4, 1283–1286.

https://doi.org/10.1021/acsmacrolett.5b00651

Lee, Y., Kim, H.J., Park, C.K., Kim, W.S., Lee, Z.H., Kim, H.H., 2012. Novel extraneural role of neurite outgrowth inhibitor A: Modulation of osteoclastogenesis via positive feedback regulation of nuclear factor of activated T cell cytoplasmic 1. J. Bone Miner. Res. 27, 1043–1054. https://doi.org/10.1002/jbmr.1561

Li, B., Alonso, D.O., Daggett, V., 2001. The molecular basis for the inverse temperature transition of elastin. J. Mol. Biol. 305, 581–92. https://doi.org/10.1006/jmbi.2000.4306

Li, B., Qiu, T., Zhang, P., Wang, X., Yin, Y., Li, S., 2014. IKVAV regulates ERK1/2 and Akt signalling pathways in BMMSC population growth and proliferation. Cell Prolif. 47, 133–145. https://doi.org/10.1111/cpr.12094

Madduri, S., Gander, B., 2010. Schwann cell delivery of neurotrophic factors for peripheral nerve regeneration. J. Peripher. Nerv. Syst. 15, 93–103. https://doi.org/10.1111/j.1529-8027.2010.00257.x

Malin, S.A., Davis, B.M., Molliver, D.C., 2007. Production of dissociated sensory neuron cultures and considerations for their use in studying neuronal function and plasticity. Nat. Protoc. 2, 152–160. https://doi.org/10.1038/nprot.2006.461

Meyer, D.E., Chilkoti, a, 1999. Purification of recombinant proteins by fusion with thermally-responsive polypeptides. Nat. Biotechnol. 17, 1112–1115. https://doi.org/10.1038/15100

Meyer, D.E., Chilkoti, A., 2004. Quantification of the effects of chain length and concentration on the thermal behavior of elastin-like polypeptides. Biomacromolecules 5, 846–851. https://doi.org/10.1021/bm034215n

Miao, M., Cirulis, J.T., Lee, S., Keeley, F.W., 2005. Structural determinants of cross-linking and hydrophobic domains for self-assembly of elastin-like polypeptides. Biochemistry

44, 14367–75. https://doi.org/10.1021/bi0510173

Nakamura, M., Mie, M., Mihara, H., Nakamura, M., Kobatake, E., 2008. Construction of
multi-functional extracellular matrix proteins that promote tube formation of endothelial
cells. Biomaterials 29, 2977–2986. https://doi.org/10.1016/j.biomaterials.2008.04.006

Nettles, D.L., Chilkoti, A., Setton, L.A., 2010. Applications of elastin-like polypeptides in
tissue engineering. Adv. Drug Deliv. Rev. 62, 1479–1485.
https://doi.org/10.1016/j.addr.2010.04.002

Nettles, D.L., Kitaoka, K., Hanson, N.A., Flahiff, C.M., Mata, B.A., Hsu, E.W., Chilkoti, A.,
Setton, L.A., 2008. In situ crosslinking elastin-like polypeptide gels for application to
articular cartilage repair in a goat osteochondral defect model. Tissue Eng. Part A 14,
1133–40. https://doi.org/10.1089/ten.tea.2007.0245

Nicol, a, Gowda, D.C., Urry, D.W., 1992. Cell adhesion and growth on synthetic elastomeric
matrices containing Arg-Gly-Asp-Ser-3. J. Biomed. Mater. Res. 26, 393–413.
https://doi.org/10.1002/jbm.820260309

Niece, K.L., Czeisler, C., Sahni, V., Tysseling-Mattiace, V., Pashuck, E.T., Kessler, J.A.,
Stupp, S.I., 2008. Modification of gelation kinetics in bioactive peptide amphiphiles.
Biomaterials 29, 4501–9. https://doi.org/10.1016/j.biomaterials.2008.07.049

Nomizu, M., Weeks, B.S., Weston, C.A., Kim, W.H., Kleinman, H.K., Yamada, Y., 1995.
Structure-activity study of a laminin α1 chain active peptide segment Ile-Lys-Val-Ala-
Val (IKVAV). FEBS Lett. 365, 227–231. https://doi.org/10.1016/0014-5793(95)00475-
O

Pasut, G., Veronese, F.M., 2007. Polymer–drug conjugation, recent achievements and general
strategies. Prog. Polym. Sci. 32, 933–961.

https://doi.org/10.1016/J.PROGPOLYMSCI.2007.05.008

Prieto, S., Shkilnyy, A., Rumplasch, C., Ribeiro, A., Arias, F.J., Rodríguez-Cabello, J.C.,
Taubert, A., 2011. Biomimetic calcium phosphate mineralization with multifunctional
elastin-like recombinamers. Biomacromolecules 12, 1480–1486.
https://doi.org/10.1021/bm200287c

Santiago, L.Y., Nowak, R.W., Peter Rubin, J., Marra, K.G., 2006. Peptide-surface
modification of poly(caprolactone) with laminin-derived sequences for adipose-derived
stem cell applications. Biomaterials 27, 2962–9.
https://doi.org/10.1016/j.biomaterials.2006.01.011

Shekaran, A., Garcia, A.J., 2011. Nanoscale engineering of extracellular matrix-mimetic
bioadhesive surfaces and implants for tissue engineering. Biochim. Biophys. Acta 1810,
350–60. https://doi.org/10.1016/j.bbagen.2010.04.006

Silva, D.I., Santos, B.P. Dos, Leng, J., Oliveira, H., Amédée, J., 2017. Dorsal root ganglion
neurons regulate the transcriptional and translational programs of osteoblast
differentiation in a microfluidic platform. Cell Death Dis. 8, 3209.
https://doi.org/10.1038/s41419-017-0034-3

Silva, G.A., Czeisler, C., Niece, K.L., Beniash, E., Harrington, D.A., Kessler, J.A., Stupp,
S.I., 2004. Selective Differentiation of Neural Progenitor Cells by High – Epitope
Density Nanofibers. Science (80-.). 303, 1352–1355.
https://doi.org/10.1126/science.1093783

Testera, A.M., Girotti, A., de Torre, I.G., Quintanilla, L., Santos, M., Alonso, M., Rodríguez-
Cabello, J.C., 2015. Biocompatible elastin-like click gels: design, synthesis and
characterization. J. Mater. Sci. Mater. Med. 26, 105. https://doi.org/10.1007/s10856-

015-5435-1

Trabbic-carlson, K., Setton, L.A., Chilkoti, A., 2003. Swelling and Mechanical Behaviors of Chemically Cross-Linked Hydrogels of Elastin-like Polypeptides Swelling and Mechanical Behaviors of Chemically Cross-Linked Hydrogels of Elastin-like Polypeptides. Society 572–580. https://doi.org/10.1021/bm025671z

Urry, D.W., 1992. Free energy transduction in polypeptides and proteins based on inverse temperature transitions. Prog. Biophys. Mol. Biol. 57, 23–57. https://doi.org/10.1016/0079-6107(92)90003-O

Urry, D.W., Trapane, T.L., Prasad, K.U., 1985. Phase-structure transitions of the elastin polypentapeptide-water system within the framework of composition-temperature studies. Biopolymers 24, 2345–2356. https://doi.org/10.1002/bip.360241212

Wang, H., Cai, L., Paul, A., Enejder, A., Heilshorn, S.C., 2014. Hybrid elastin-like polypeptide-polyethylene glycol (ELP-PEG) hydrogels with improved transparency and independent control of matrix mechanics and cell ligand density. Biomacromolecules 15, 3421–8. https://doi.org/10.1021/bm500969d

Wilkins, A., Kemp, K., Ginty, M., Hares, K., Mallam, E., Scolding, N., 2009. Human bone marrow-derived mesenchymal stem cells secrete brain-derived neurotrophic factor which promotes neuronal survival in vitro. Stem Cell Res. 3, 63–70. https://doi.org/10.1016/J.SCR.2009.02.006

Xu, D., Asai, D., Chilkoti, A., Craig, S.L., 2012. Rheological Properties of Cysteine-Containing Elastin-Like Polypeptide Solutions and Hydrogels. Biomacromolecules 13, 2315–2321. https://doi.org/10.1021/bm300760s

Yamada, M., Kadoya, Y., Kasai, S., Kato, K., Mochizuki, M., Nishi, N., Watanabe, N.,

Kleinman, H.K., Yamada, Y., Nomizu, M., 2002. Ile-Lys-Val-Ala-Val (IKVAV)-
containing laminin α1 chain peptides form amyloid-like fibrils. FEBS Lett. 530, 48–52.
https://doi.org/10.1016/S0014-5793(02)03393-8

Yu, L.M.Y., Kazazian, K., Shoichet, M.S., 2007. Peptide surface modification of
methacrylamide chitosan for neural tissue engineering applications. J. Biomed. Mater.
Res. A 82, 243–55. https://doi.org/10.1002/jbm.a.31069

Zhang, Y.N., Avery, R.K., Vallmajo-Martin, Q., Assmann, A., Vegh, A., Memic, A., Olsen,
B.D., Annabi, N., Khademhosseini, A., 2015. A Highly Elastic and Rapidly
Crosslinkable Elastin-Like Polypeptide-Based Hydrogel for Biomedical Applications.
Adv. Funct. Mater. 25, 4814–4826. https://doi.org/10.1002/adfm.201501489

Zhu, J., 2010. Bioactive Modification of Poly(ethylenglykol) Hydrogels for Tissue
Engineering. Biomaterials 31, 4639–4656.
https://doi.org/10.1016/j.biomaterials.2010.02.044.Bioactive

Figure 1

```
atgtgcgttccgggtgttggtgttccgggtatcggtgttccgggtatgggtgttccgggt
 M  C  V  P  G  V  G  V  P  G  I  G  V  P  G  M  G  V  P  G
attggggtaccgggtgttggtatcaaagttgcggttgttccgggtgttggtgttccgggt
 I  G  V  P  G  V  G [ I  K  V  A  V] V  P  G  V  G  V  P  G
attggtgttccgggtatgggtgttccgggtatcggtgttccgggtgttggtgttccgggt
 I  G  V  P  G  M  G  V  P  G  I  G  V  P  G  V  G  V  P  G
gttggtgttccgggtattggtgttccgggtatgggtgttccgggtattggtgttccgggt
 V  G  V  P  G  I  G  V  P  G  M  G  V  P  G  I  G  V  P  G
gttggtatcaaagttgcggttgttccgggtgttggtgttccgggtattggtgttccgggt
 V  G [ I  K  V  A  V] V  P  G  V  G  V  P  G  I  G  V  P  G
atgggtgttccgggtatcggtgttccgggtgttggttgggttccatgctaa
 M  G  V  P  G  I  G  V  P  G  V  G  W  V  P  C  -
```

Figure 1: Schematic representation of the nucleic acid and protein sequences of ELP-IKVAV. Methionine residues are in bold, the two cysteine residues are in bold underlined, and the tryptophan residue is in bold italic. The two pentapeptide IKVAV sequences are boxed. The ELP-VKAIV polypeptide differs from this sequence by the replacement of the two IKVAV motifs by two VKAIV sequences.

Figure 2
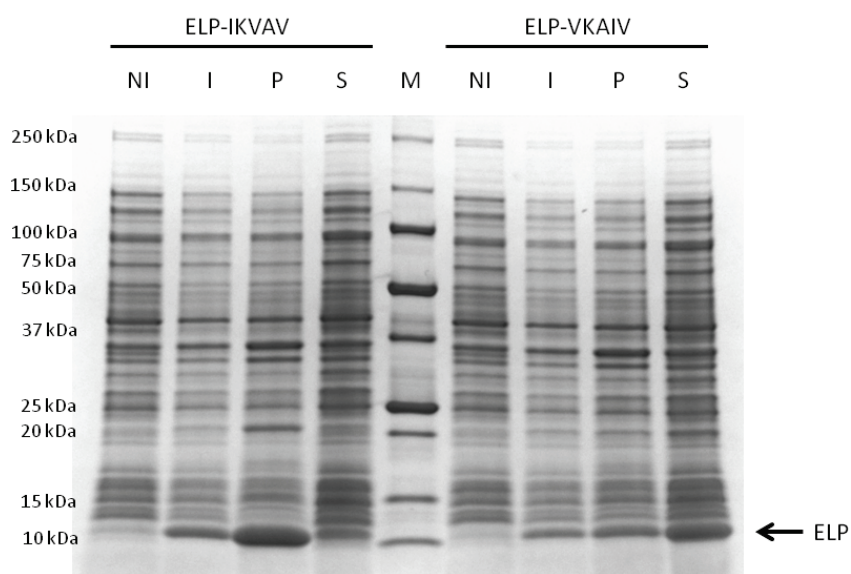
Figure 2: SDS-PAGE (4-20%) analysis of the protein fractions obtained during the purification process.

NI, total protein extract from non-induced culture; I, total proteins extract from a culture 21 h after IPTG induction; P: pellet 3,000 g obtained after cell lysis; S: supernatant 3,000 g obtained after cell lysis; M: Precision Plus Protein Standards. InstantBlue[TM] was used to stain the gel. The loading sample buffer contained 0.68 M β-mercaptoethanol as reducing agent. Bands appearing at the expected MW of ELPs are indicated by an arrow.

Figure 3
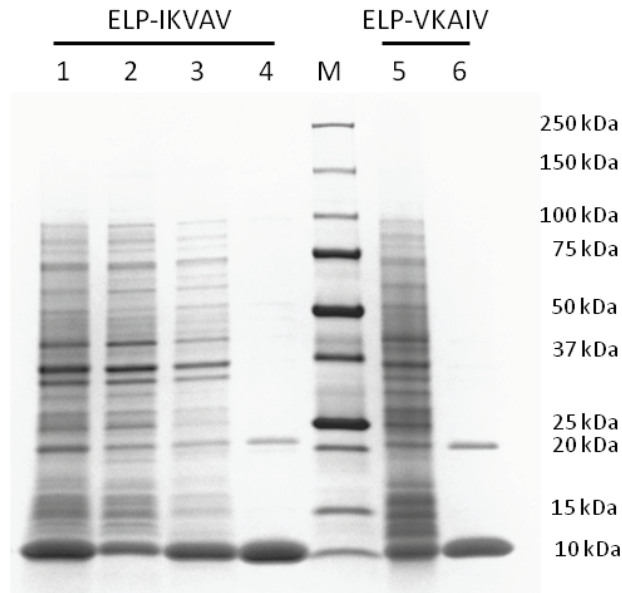
Figure 3: SDS-PAGE (4-20%) analysis of the protein fractions obtained with the optimized purification process.

After culture of the ELP clones, cells were recovered by centrifugation and lysed by sonication. After centrifugation at 3,000 g, the insoluble pellet containing the ELP-IKVAV was mixed with a solution of PBS containing β-mercaptoethanol (0.68 M final concentration). After an overnight incubation on a rotator at 4° C, the homogenates were centrifuged at 3,000 g for 10 min at 4° C. Supernatants were used for ITC purification. For ELP-VKAIV, ITC purification was performed directly on the 3,000 g supernatant obtained after cell lysis. 1: pellet 3,000 g post-lysis; 2: pellet 3,000 g post-incubation with β-mercaptoethanol; 3: supernatant 3,000 g post-incubation with β-mercaptoethanol; 4 purified ELP after three rounds of ITC; 5 supernatant 3 000 g post-lysis; 6: purified ELP-VKAIV after four rounds of ITC; M: Precision Plus Protein Standards. 8 μL of each protein sample were loaded in the lanes. Total volume of the fractions was 10 mL for samples 1, 2, 3 and 5

and 5 mL for samples 4 and 6. The loading sample buffer contained 0.68 M β-mercaptoethanol as reducing agent. InstantBlue[TM] was used to stain the gel.

Figure 4
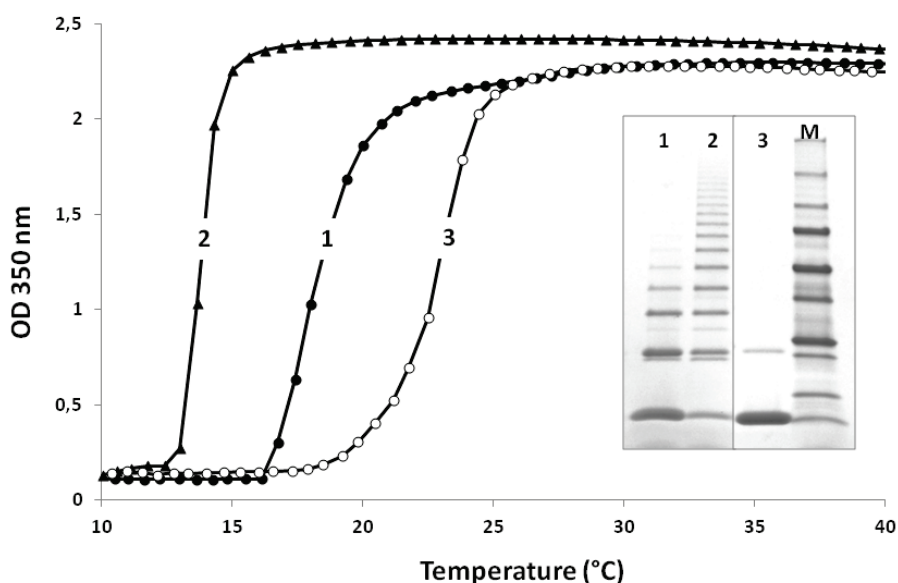
Figure 4. Turbidity profiles of ELP-VKAIV samples with different state of aggregation levels in PBS monitored by absorbance at 350 nm. Transition temperatures (Tts) were determined by measuring the turbidity at 350 nm in PBS at a scan rate of 1 °C/min. Sample concentration was 90 µM. Solid triangles: sample pre-heated for 10 min at 95°C before the experiment; solid circles: non-reduced sample; open circles: sample containing 0.68 M β-mercaptoethanol. Insert: SDS-PAGE analysis of 10 µL of the samples used for the turbidity profile analysis. Lane 1, non-reduced sample; lane 2: pre-heated sample (10 min at 95° C); lane 3: reduced sample; M: Precision Plus Protein Standards. InstantBlue[TM] was used to stain the gel.

Figure 5
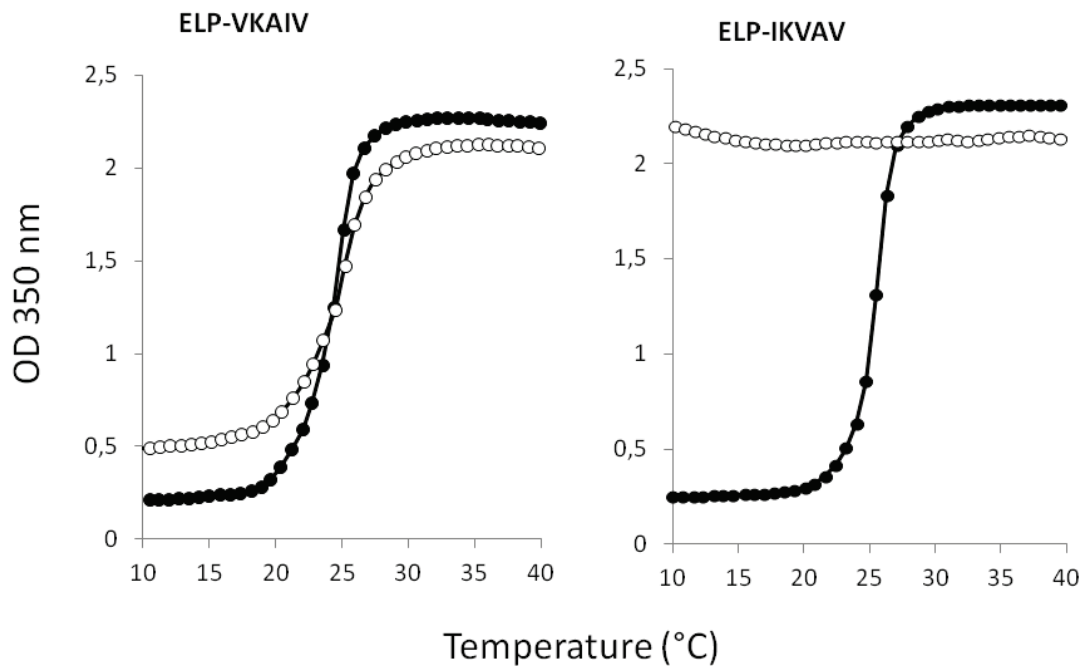
Figure 5. Turbidity profiles monitored by absorbance at 350 nm of ELPs in PBS supplemented with 0.68 M β-mercaptoethanol. Transition temperatures (Tts) were determined by measuring the turbidity at 350 nm at a scan rate of 1 °C/min. The ELPs concentration was 60 µM. Solid circles = data from the first temperature ramp from 15°C to 40°C, open circles = data from the second temperature ramp for the same sample.

Figure 6
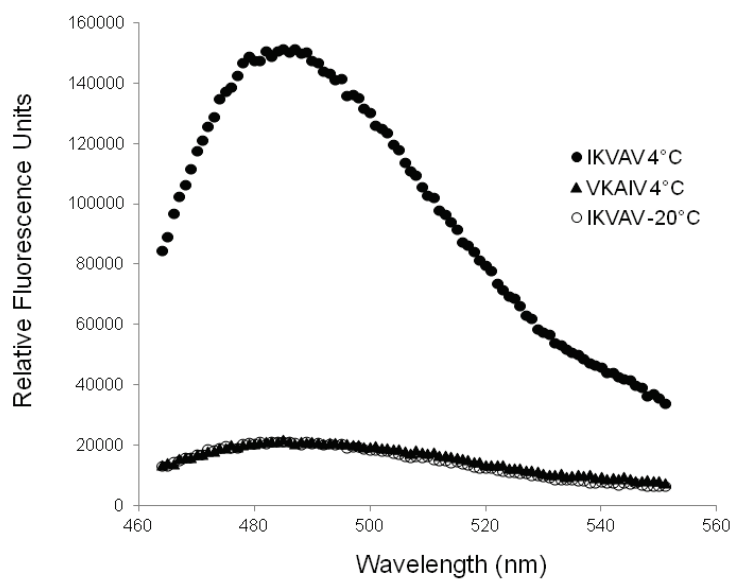
Figure 6. Amyloid formation monitored by ThT binding. Emission spectrum (between 460 and 550 nm) of Tht (20 µM) was recorded in presence of 150 µM ELP. The wavelength of excitation was 440-448 nm. ELP-IKVAV stored for three days at 4 °C (solid circles) or stored at -20 °C (open circles), ELP-VKAIV stored for three days at 4 °C (solid triangles).
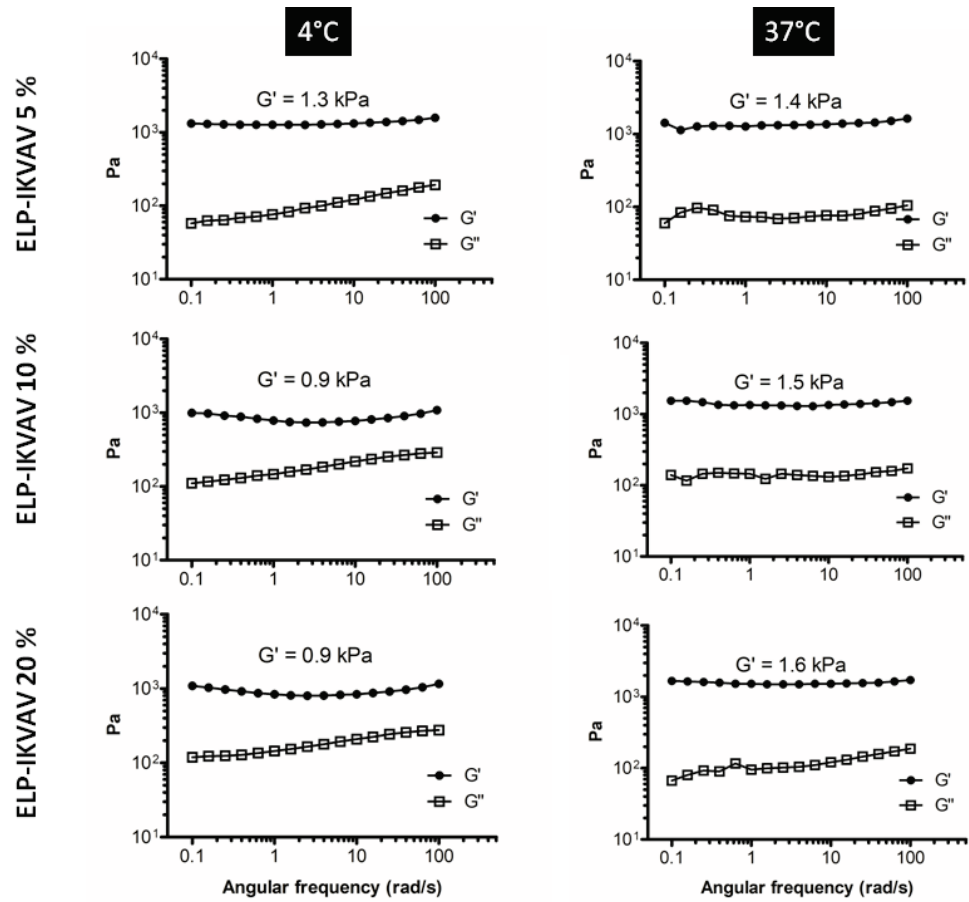
Figure 7. Rheological characterization of 15% (w/v) hydrogels but varying the ELP final concentration (w/v), namely 5, 10 and 20% (w/w), at 4, 25 and 37 °C.

All graphics show storage (G') and loss (G") moduli.

Figure 8
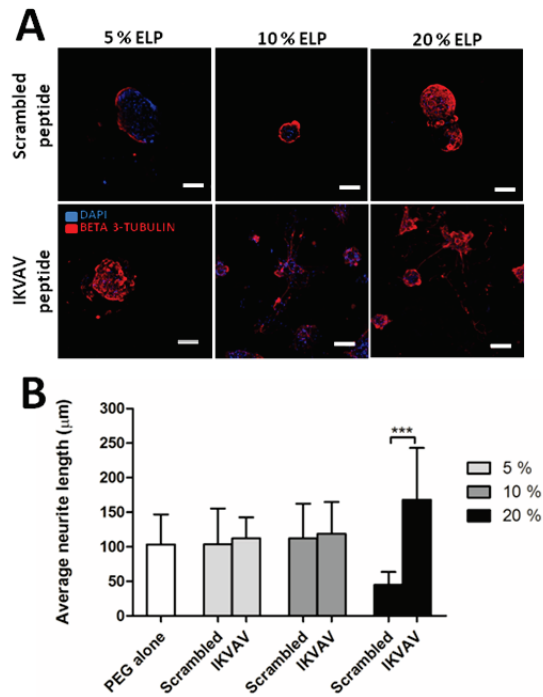
Figure 8. Sensory neurons growth on hydrogels

A) Sensory neurons morphology after 7 days of culture on PEG hydrogels, or on hydrogels
containing 5, 10 and 20% (w/w) of ELP-IKVAV or ELP-VKAIV. SNs were labeled using β
III tubulin immunostaining (red) and DAPI (blue) (bar = 100 μm). B) Average neurite length
evaluation measured after 7 days of culture on the hydrogels, containing 0, 5, 10 and 20%
(w/v) of ELP-IKVAV or ELP-VKAIV (n>4) (***indicates p< 0.001).
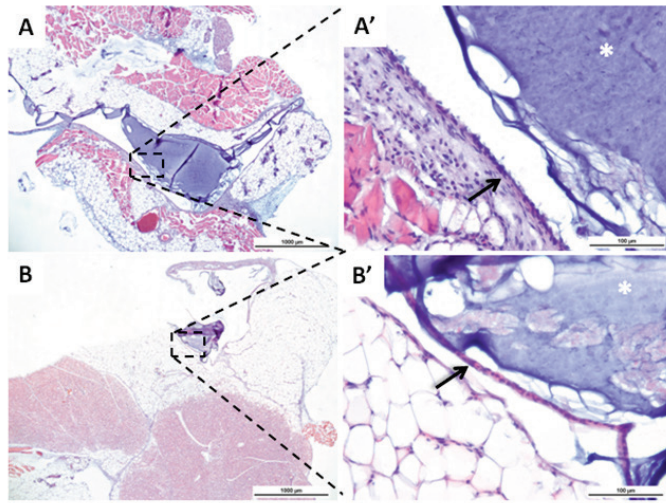
Figure 9. In vivo evaluation of cytoxicity

HE histological staining after 4 weeks of subcutaneous implantation of 20% (w/w) ELP containing the (A and A') scrambled VKAIV, and (B and B') IKVAV adhesion sequence. A' and B' are magnification of A and B, respectively. Black arrows show thin fibrous capsule tissue, and white asterisks show the hydrogel structure.

Supplementary Figures

Production, purification and characterization of an elastin-like polypeptide containing the Ile-Lys-Val-Ala-Val (IKVAV) peptide for tissue engineering applications

Bruno Paiva dos Santos[1], Bertrand Garbay[2*], Mattia Pasqua[1], Elsa Chevron[1], Zoeisha S. Chinoy[2], Christophe Cullin[3], Katell Bathany[3], , Sébastien Lecommandoux[2], Joëlle Amédée[1], Hugo Oliveira[1] and Elisabeth Garanger[2]

Figure S1: SDS-PAGE (4-20%) analysis of the protein fractions obtained during ITC purification of ELP-IKVAV from the 3,000 g supernatant.
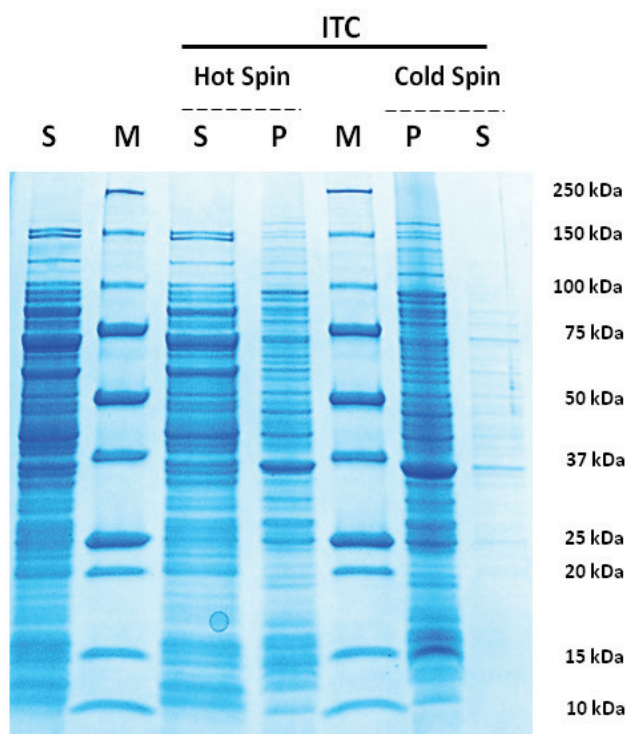
After culture of the ELP-IKVAV clone, cells were recovered by centrifugation and lysed by sonication. After centrifugation at 3,000 g, the supernatant was used for one round of ITC purification. ELP was precipitated from the 3,000 g supernatant at 37 °C in the presence of 1 M NaCl, and pelleted by centrifugation at 10,000 g and 25 °C for 10 min ("Hot Spin"). After re-suspension of the pellet in cold PBS buffer, the ELP was re-dissolved whereas insoluble proteins from *E. coli* were eliminated by centrifugation for 10 min at 10,000 g and 4 °C ("Cold Spin"). S: supernatant; P: pellet; M: Precision Plus Protein Standards. InstantBlue[TM] was used to stain the gel.

Figure S2: SDS-PAGE (4-20%) analysis of the protein fractions obtained during the purification process.
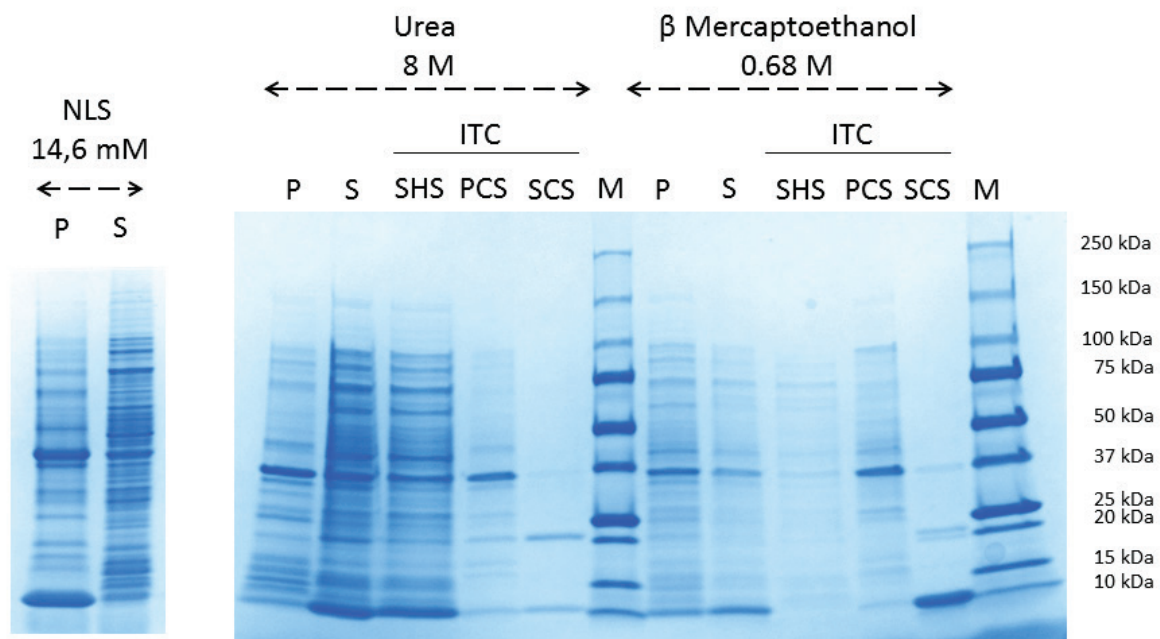
After culture of the ELP-IKVAV clone, cells were recovered by centrifugation and lysed by sonication. After centrifugation at 3,000 g, the insoluble pellet containing the ELP-IKVAV was either mixed with a solution of *N*-Lauroylsarcosine 14.6 mM (NLS), of urea 8 M or a

solution of PBS containing β-mercaptoethanol (0.68 M final concentration). After overnight incubation on a rotator at 4°C, the homogenates were centrifuged at 3,000 g for 10 min at 4° C. Supernatants were used for ITC purification (one round of purification). P: pellet 3,000 g after incubation with NLS, urea or β-mercaptoethanol; S: supernatant 3,000 g after incubation with NLS, urea or β-mercaptoethanol; SHS: supernatant of the "Hot Spin" step; PCS: pellet of the "Cold Spin" step; SCS: supernatant of the "Cold Spin" step; M: Precision Plus Protein Standards (corresponding MW are indicated on the figure). InstantBlue[TM] was used to stain the gel. Total volumes of the fractions were 1 mL for P and S, 300 µL for SHS, PCS and SCS. 10 µL of each fraction were loaded onto the gel.

**Figure S3: SDS-PAGE (4-20%) analysis of the purified ELPs under reducing or non-reducing conditions.**
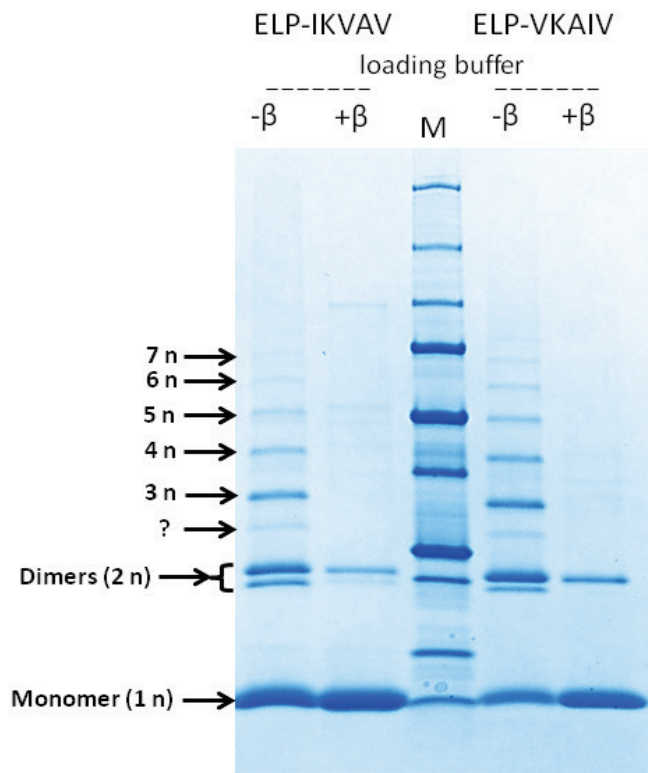
10 µg of purified ELP-IKVAV and ELP-VKAIV were incubated in the gel loading buffer with or without β-mercaptoethanol (0.68 M final concentration). After heating for 5 min at 95 °C, samples were loaded onto the gel. M: Precision Plus Protein Standards. InstantBlue[TM] was used to stain the gel. The two forms of dimers probably correspond to dimers formed respectively by one or two disulfide bridges.

**Figure S4. Mass spectrometry analyses of ELPs.**
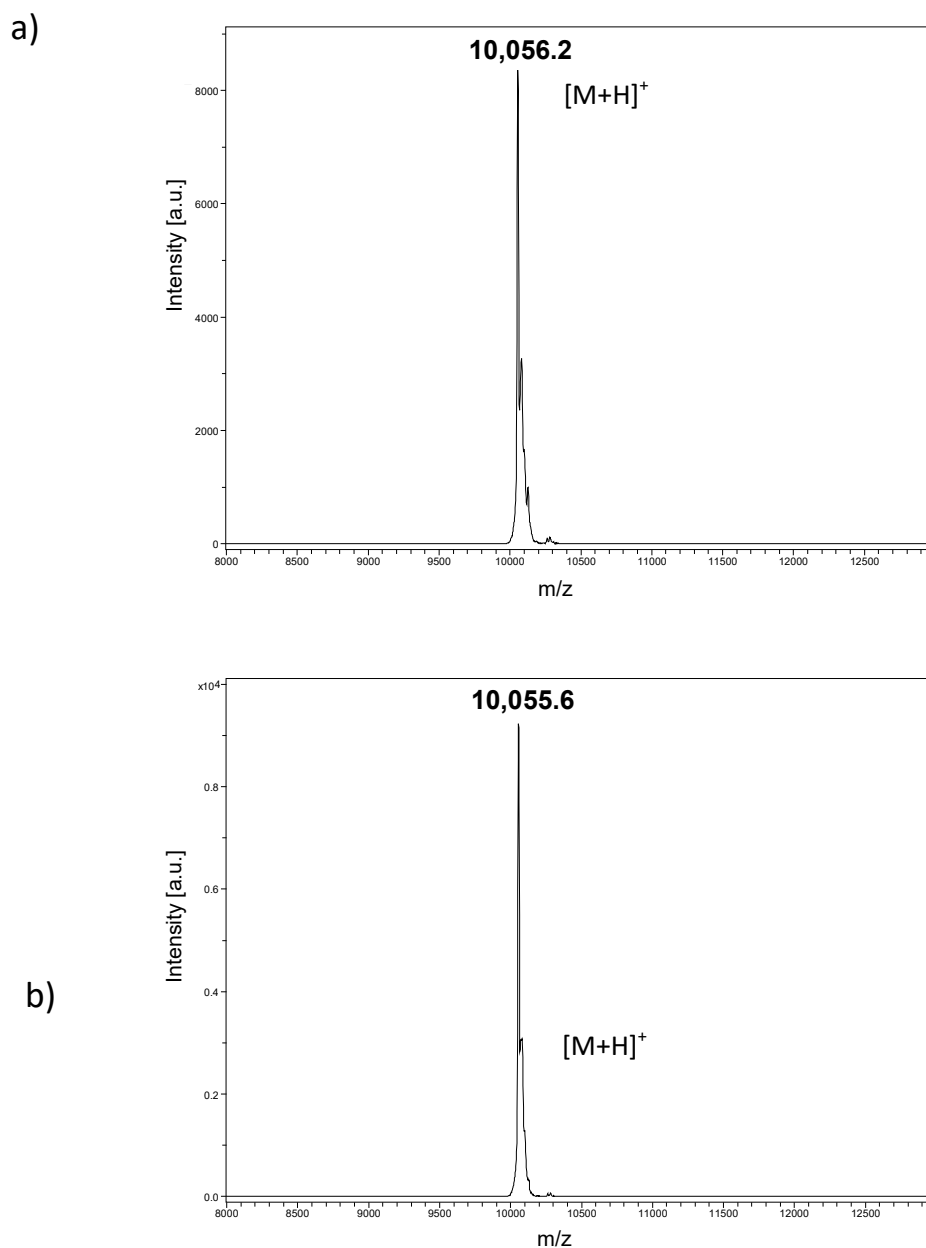
a)

b)

The molecular mass of each purified ELP was determined by matrix-assisted laser desorption/ionization mass spectrometry (MALDI-MS). MALDI MS spectra of a) ELP-IKVAV and b) ELP-VKAIV.

Figure S5. Turbidity profiles of reduced and oxidized ELP-IKAV in PBS monitored by absorbance at 350 nm.
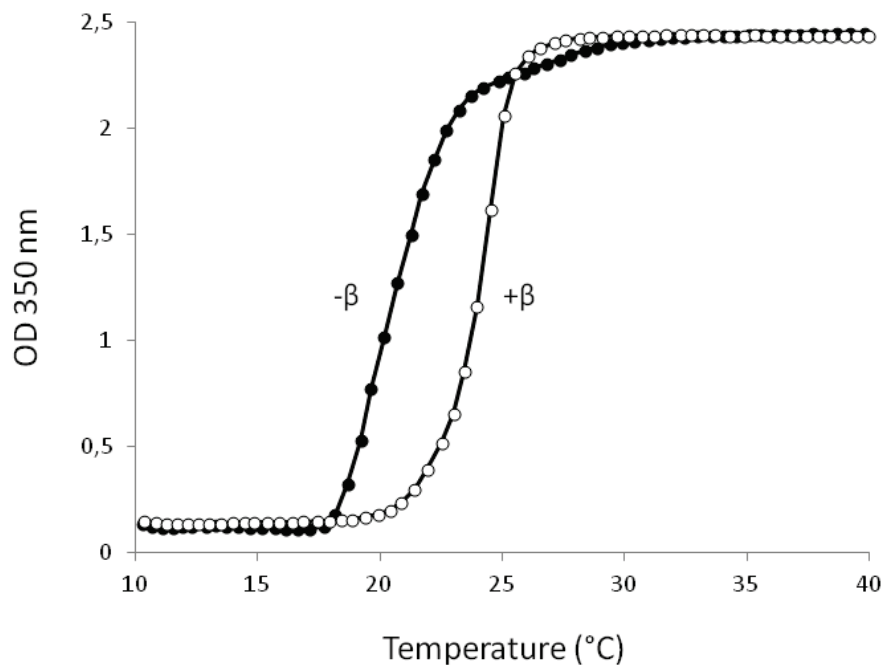

Transition temperatures (Tt) were determined by measuring the turbidity at 350 nm between 10 and 40°C at a scan rate of 1 °C/min. Optical density (OD) data is converted to a percentage of the maximum OD measured. Sample concentration was 90 μM. Solid circles: non–reduced sample. Open circles: sample containing β-mercaptoethanol (0.68 M final concentration).

Figure S6. Precipitate formation in a tube containing 150 μM ELP-IKVAV.
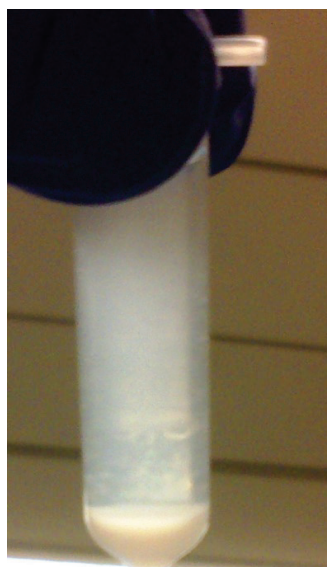
The solution was incubated overnight at 37 °C.

Figure S7. Rheological properties of ELP-VKAIV hydrogels
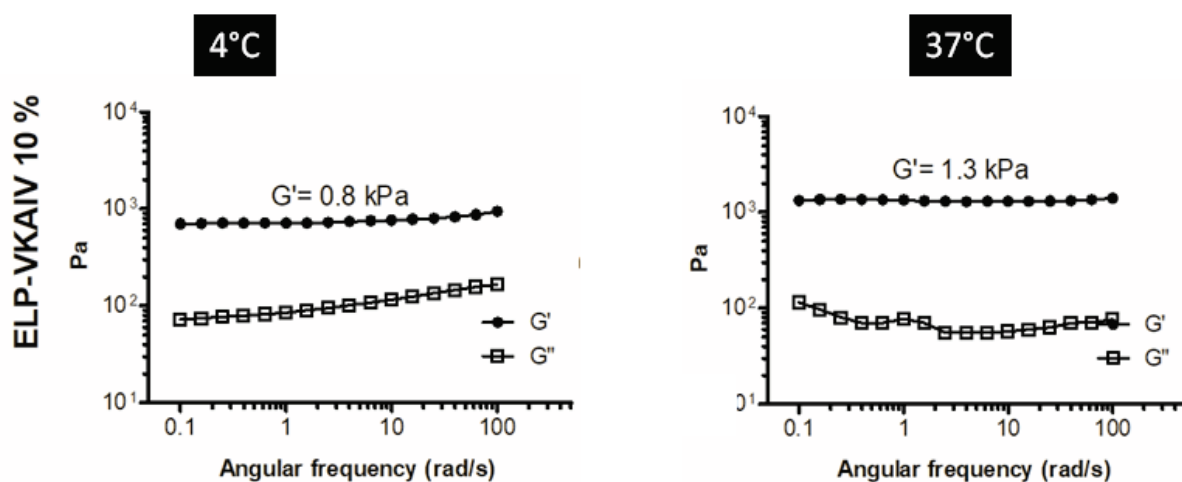
The rheological properties of the hydrogels were evaluated after 24 h of soaking in PBS by

determining the frequency dependence of the storage (G') and loss moduli (G"). Frequency

sweeps were performed at a constant strain (0.1) in the angular frequency range 0.1–100 rad s^{-1}. This characterization was performed for the composite hydrogels at a final concentration of 15 % (w/v) while the ELP concentration in the final hydrogel mass was 10 % (w/w). Measures were performed at 4 and 37 °C.